ELSEVIER

Catalysis Today 76 (2002) 75–86

CATALYSIS TODAY

www.elsevier.com/locate/cattod

Hydrogen production from biomass gasification on nickel catalysts Tests for dry reforming of methane

C. Courson, L. Udron, D. Świerczyński, C. Petit, A. Kiennemann*

Laboratoire de Matériaux, Surfaces et Procédés pour la Catalyse, ECPM-UMR 7515, 25 rue Becquerel, 67087 Strasbourg Cedex 02, France

Abstract

Ni–olivine catalyst used for increasing hydrogen production in fluidised bed biomass gasification has been optimised. Performance of the system in methane dry reforming has been studied as a function of nickel content, precursor salt, and calcination temperature. The optimised catalyst was prepared from nickel nitrate and contained more than 5 wt.% of nickel oxide on olivine after calcination at 1100 °C. Ni–support initial interactions were studied by means of XRD, SEM, TEM–EDXS and TPR. Nickel oxide is strongly linked to olivine, in form of grafts and is still reducible under catalytic test. With a CH_4/CO_2 ratio of 1, methane conversion and hydrogen yield were 95% after 80 h of test at 800 °C. Very good stability of this catalyst during ageing can be explained by absence of nickel particles sintering and very low carbon content observed after catalytic tests. This catalyst meets all the requirements of activity, stability and attrition resistance for use in the fluidised bed biomass gasification process.

Keywords: Biomass gasification; Dry reforming of methane; Nickel catalysts

1. Introduction

Biomass as a source of renewable energy presents at least one main advantage over fossil fuels: lower emission of carbon dioxide and other greenhouse gases. In particular, hydrogen production from biomass for fuel cells application is very attractive [1] and this process has been optimised in fluidised bed conditions [2–4].

Developments in fluidised bed technology necessitate adaptation of catalytic bed materials. The catalyst has to be strong enough to resist attrition in addition of having a similar density as the biomass to be fluidised in the same conditions. Sand is the most popular material used in this case but plays no active role in biomass gasification. Natural olivine, an orthosilicate of iron and magnesium, meets the requirements of activity, resistance and density [5].

Biomass steam gasification leads to a mixture containing water, hydrogen, carbon oxides and small amount of methane and higher hydrocarbons. This mixture can be enriched in hydrogen by catalytic light hydrocarbons reforming with water or carbon dioxide. Both are present in the mixture and both can be used as oxidants.

For economic reasons nickel catalyst is the most suitable choice among metals like Co, Fe, Pt, Ru and Rh. Ni on Al_2O_3 or MgO favours syngas production with high H_2/CO molar ratio but, when used at high temperatures, sintering of nickel particles and carbon deposition occurs [6–9]. However, it has been demonstrated that strong interactions between nickel oxide and some supports [10] or well-defined structure, like perovskite [11,12], limited nickel sintering.

* Corresponding author. Tel.: +33-390-2427-66; fax: +33-390-2427-68.
E-mail address: kiennemann@chimie.u-strasbg.fr (A. Kiennemann).

0920-5861/02/$ – see front matter
PII: S0920-5861(02)00202-X

Basic olivine used as nickel support can be an attractive solution for biomass gasification. Moreover, natural olivine contains iron, which can stabilise nickel in the support structure [11,12]. The initial nickel–olivine interactions have to be strong enough to prevent nickel sintering and attrition of the active phase. Moreover, to be active for methane reforming, nickel particles must be accessible. Nickel strongly linked to the olivine support has previously been highlighted as a material meeting the requirements of use in fluidised bed gasifier [13]. The aim of this paper is to show that olivine can be an interesting support for nickel, giving a system with high attrition resistance and strong linking with nickel.

The present work firstly shows characterisation of olivine support and its evolution with calcination temperature. Secondly in order to optimise the nickel–olivine catalyst, the effect of three parameters (nickel content, nickel precursors and calcination temperature) is investigated. Finally the efficiency and the stability of catalysts is determined for the dry reforming of methane.

2. Experimental procedure

2.1. Olivine as catalyst support

Natural olivine is produced from an Austrian mine and its composition (30.5 wt.% of Mg, 7.1 wt.% of Fe and 19.6 wt.% of Si), obtained by atomic adsorption, leads to the mean formula $(Mg_{0.92}Fe_{0.08})_2SiO_4$ with an iron excess (0.7 wt.%) in the form of free iron oxide. The material already contains small amounts of nickel as well as Ca, Al and Cr (lower than 0.2 wt.% each).

The specific surface area of the olivine is very low ($<1\,m^2/g$). Olivine samples were calcined at 900, 1100 or 1400 °C, under the same conditions as the Ni–olivine samples.

2.2. Catalyst preparation

The Ni–olivine catalysts were prepared by impregnation of natural olivine with an excess of nickel salt solution. In order to study the nickel precursor effect, nitrate, chloride and acetate salts were dissolved in water.

After water evaporation, the samples were calcined under air for 4 h at different temperatures (900, 1100 or 1400 °C).

The concentration of nickel nitrate solution was modified in order to obtain catalysts containing from 2 to 10 wt.% of NiO after calcination at 1100 °C. These different ways of preparation have permitted to obtain a series of Ni–olivine catalysts described in Table 1.

2.3. Characterisation of natural olivine and nickel–olivine catalysts

Samples were characterised by powder X-ray diffraction (XRD) on a Siemens D500TT diffractometer using Cu Kα radiation, by transmission electron microscopy (TEM) on a Topcon EM 002B apparatus coupled to energy dispersive X-ray spectroscopy

Table 1
Preparation parameters, real nickel oxide contents and Ni–olivine catalysts nomenclature

Preparation parameter	Nomenclature	Calcination temperature (°C)	NiO content (wt.%)		Nickel salt
			Theoretical	Real	
Calcination temperature	900N5%	900	5	5	Nitrate
	1100N5%	1100	5	5	Nitrate
	1400N5%	1400	5	5	Nitrate
Nickel oxide content	1100N2%	1100	2	1.9	Nitrate
	1100N5%	1100	5	5	Nitrate
	1100N6.4%	1100	6.4	5.7	Nitrate
	1100N10%	1100	10	7.4	Nitrate
Nickel salt	1100N5%	1100	5	5	Nitrate
	1100Cl5%	1100	5	4.8	Chloride
	1100A5%	1100	5	3.4	Acetate

(EDXS), by scanning electron microscopy (SEM) on a JEOL JSM 840 microscope. For the TEM analysis, the samples were grounded in a mortar then deposited on a Cu grid covered with a perforated carbon membrane. The statistical distribution of heavy elements (Si, Mg, Fe, Ni) has been obtained by microanalysis with a large window ($\phi = 200$ nm). An analysis performed on different areas of the sample with a small window ($\phi = 14$ nm) allowed monitoring of the dispersion [14]. For the SEM analysis, the sample was included into a resin and then polished for the analyses. Elementary analysis of the samples was performed in the CNRS Centre in Vernaison. Carbon formed during the catalytic tests was analysed by coulometry after combustion and then trapping of the products in an acid solution.

The active phase for methane reforming is the nickel metal. So, the reducibility of the catalysts under hydrogen gives valuable information. This has been followed by temperature programmed reduction (TPR) performed on 200 mg of catalyst placed in a U-shaped quartz tube (6.6 mm ID). The reductive gas mixture ($H_2 = 0.12\,l\,h^{-1}$ and $Ar = 3\,l\,h^{-1}$) passed through the reactor heated from room temperature to 950 °C with a slope of 15 °C min^{-1} then maintained at 950 °C until the end of H_2 consumption showed by the baseline return. A thermal conductivity detector (TCD) was used for quantitative determination of hydrogen consumption.

2.4. Catalytic tests of the nickel–olivine system

Catalytic activity and stability of the various catalysts were studied in dry reforming of methane without prior reduction.

The operating conditions were the following: fixed bed quartz reactor (6.6 mm ID); inlet temperature: 600–800 °C; total feed flow rate: $3\,l\,h^{-1}$; weight of catalyst: 200 mg; CH_4/CO_2 molar ratio: 1.

The outlet gas was analysed by two gas chromatographs used simultaneously. The first one gave the amount of remaining CH_4 and of produced CO, CO_2 separated on a carbosieve SII column (3 m; 80–100 mesh; He: 25 ml min^{-1}); the second one quantified CO and H_2 separated on a molecular sieve (5 Å; 2 m; 80–100 mesh; Ar: 18 ml min^{-1}).

Two different temperature regimes for the catalytic reaction were used. The first one, presented in Fig. 1, starts with a continuous increase of temperature, 10 °C/min, from room temperature to 500 °C and a stage at 500 °C. A “simple cycle” of the temperature consists of an increase until 800 °C and decrease to 500 °C. During the cycle, analyses by gas chromatography were made every 60 °C. At the 800 °C step (stage for 40 min), three consecutive analyses were performed.

The second temperature regime (Fig. 2), called “cycles and ageing” was composed of the initial steps and two cycles under reaction gas mixture. The first cycle was similar to the “simple cycle” described above except that the final temperature was equal to 400 °C. The two cycles were separated by a stage at 400 °C under inert gas. The second cycle was also similar to the “simple cycle” described above except that the initial and final temperatures were equal to 400 °C. Finally, the stability of the catalysts was studied under reaction gas mixture during a stage at 800 °C after an increase of 3 °C min^{-1} from 400 to 800 °C. Chromatographic analyses were performed like during the “simple cycle”.

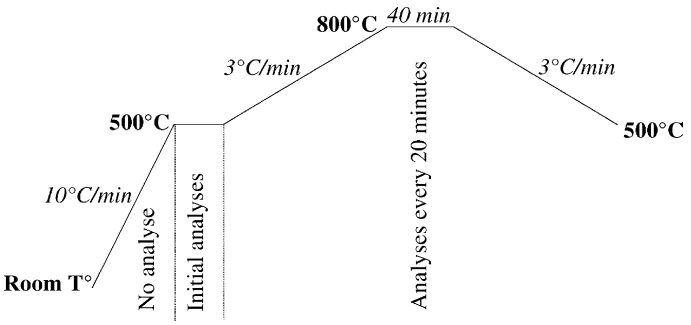

Fig. 1. “Simple cycle” temperature program for catalytic tests.

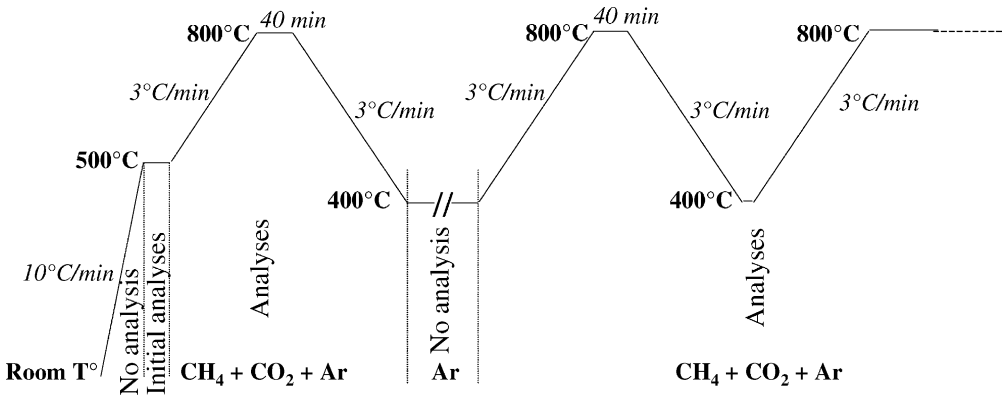

Fig. 2. "Cycle and ageing" temperature program for catalytic tests.

Given the following reaction schemes for the dry reforming:

$$CH_4 + CO_2 \rightarrow 2CO + 2H_2 \quad (1)$$

methane and carbon dioxide conversions and hydrogen and carbon monoxide yields can be calculated:

$$\text{Conversion}(CH_4)\ (\%) = \frac{(CH_4)_{in} - (CH_4)_{out}}{(CH_4)_{in}} \times 100 \quad (2)$$

$$\text{Conversion}(CO_2)\ (\%) = \frac{(CO_2)_{in} - (CO_2)_{out}}{(CO_2)_{in}} \times 100 \quad (3)$$

$$\text{Yield}(H_2)\ (\%) = \frac{(H_2)_{out}}{(CH_4)_{in}} \times \frac{100}{2} \quad (4)$$

$$\text{Yield}(CO)\ (\%) = \frac{(CO)_{out}}{(CH_4)_{in} + (CO_2)_{in}} \times 100 \quad (5)$$

3. Results and discussion

3.1. Characterisation of the nickel–olivine initial interactions

3.1.1. Influence of calcination temperature on the natural olivine

Natural olivine was calcined at 900, 1100 or 1400 °C. XRD of olivine without pre-treatment show that the main lines are close to those of the Mg_2SiO_4 forsterite (34-0189 JCPDS file) [15]. Natural olivine and forsterite are then isomorphic. The secondary crystalline phases observed are the (Mg, Fe) SiO_3 phase (19-0606 JCPDS file) visualised by its 100-intensity line at 28.2° (2θ) [16] and Fe_2O_3 and Fe_3O_4. The (Mg, Fe) SiO_3 phase is due to a modification of the Mg_2SiO_4 forsterite phase at high temperature. XRD of natural olivine presents differences in the intensities of the reflections depending on the sample. After calcination at 900 and 1100 °C, crystalline phases close to that of the natural olivine with almost no change of line positions and global intensities resulted. After calcination at higher temperatures, the intensities of the strongest lines of the secondary phases (Mg, Fe) SiO_3 and Fe_3O_4 increase without depending on the sample.

Analyses by EDXS were performed on various areas of the sample with both large (200 nm) and small (14 nm) windows. Overall, there is no difference in the elemental distribution of particulates between data collected by small and large windows. Some free iron particles are however present as shown in samples 9–11 of Fig. 3.

SEM performed for olivine calcined at various temperatures confirms the presence of iron-rich areas in the whole depth of the grains. In fact, the bright areas can be associated to iron-rich areas on olivine calcined at 900 °C (Fig. 4). After calcination at 1400 °C, olivine presents more iron-rich areas as if calcination has led to extraction of iron oxide from the olivine structure.

TPR was performed on olivine without pre-treatment and on olivine calcined at 900, 1100 and 1400 °C

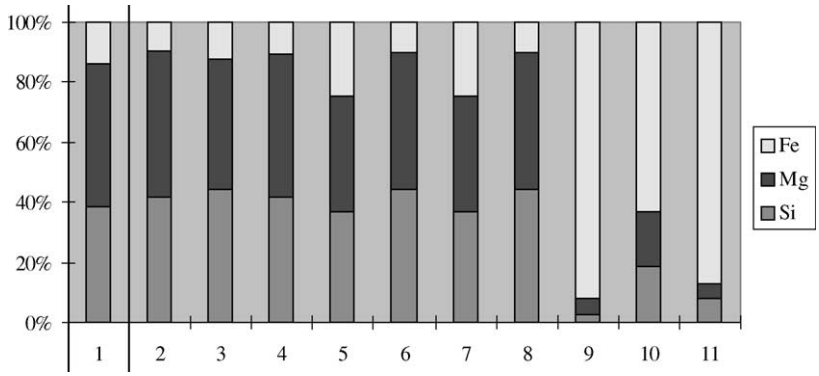

Fig. 3. Analysis obtained by energy dispersive X-ray spectrometry (bar 1 = 200 nm, bars 2–11 = 14 nm).

(Fig. 5). Reduction profiles for these samples are similar and only one reduction peak between 650 and 710 °C can be seen. This broad peak is attributed to the reduction of the free iron oxide associated to the olivine structure. Earlier work in our laboratory [12] has shown that iron inserted in a well-defined structure as oxide cannot be reduced at temperatures lower than 900 °C. The shoulder observed at this temperature can be associated with the reduction of the various oxides of olivine structure. This reduction is very slow and would continue after 950 °C, the highest temperature of our reduction study.

The only difference in the hydrogen consumption of these four samples is the intensity and the width of their reduction peak. The higher the calcination temperature, the more intense and broad this peak is. In fact, this phenomenon is the most visible between the samples calcined at 1100 and 1400 °C. Free iron oxide content increases with calcination temperature as observed by SEM and XRD.

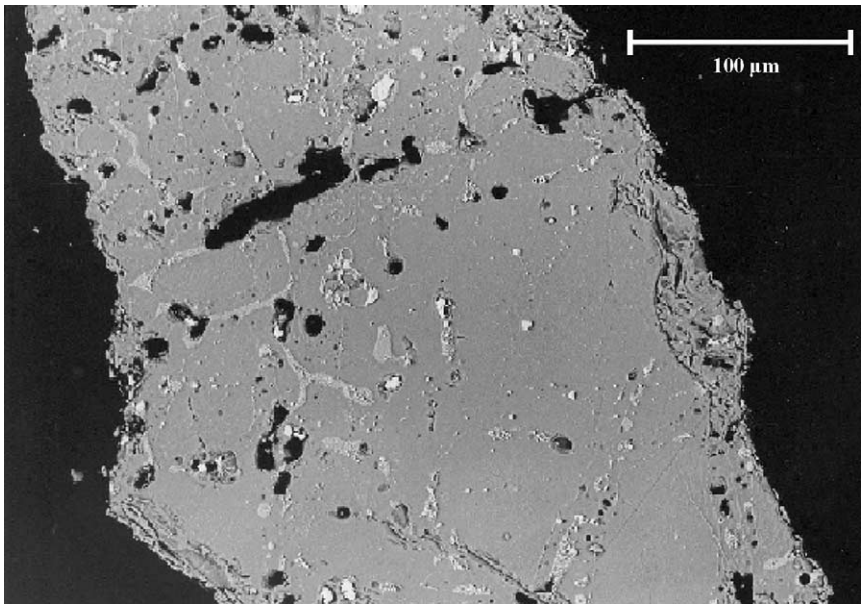

Fig. 4. SEM (back-scattered electrons) of olivine calcined at 900 °C.

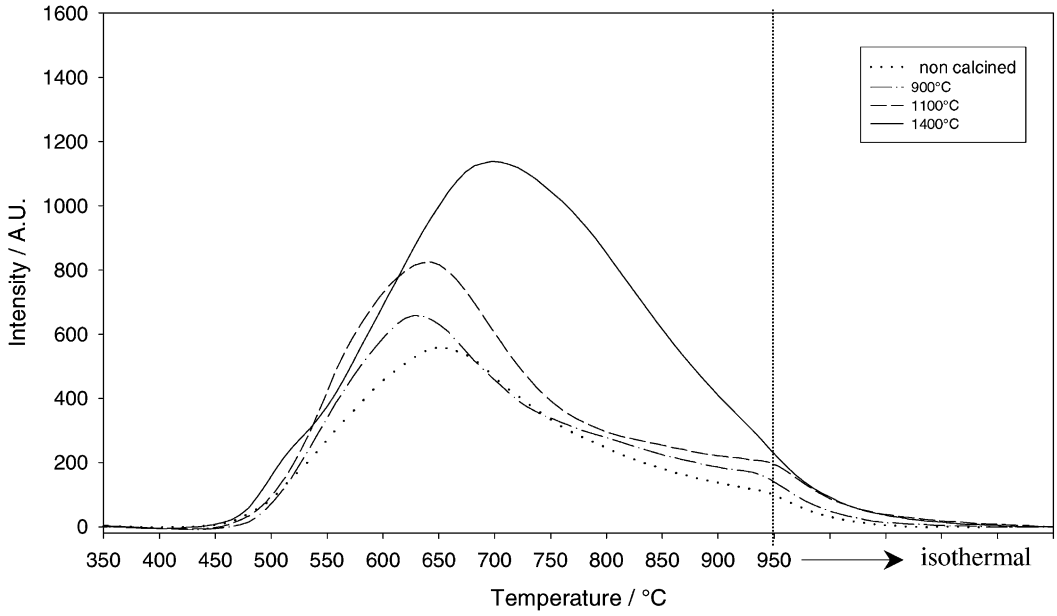

Fig. 5. TPR of natural olivine without pre-treatment and calcined at 900, 1100 and 1400 °C.

3.1.2. Influence of calcination temperature on the nickel–olivine catalysts

Firstly, olivine was impregnated with an aqueous solution of nitrate salt in order to obtain samples containing 5 wt.% of nickel oxide. These samples were calcined at 900 °C (900N5%), 1100 °C (1100N5%) or 1400 °C (1400N5%). The XRD of these three samples are presented together with that of olivine calcined at 1400 °C (Fig. 6). The main lines of natural olivine close to those of the Mg_2SiO_4 forsterite are maintained indicating that the support is not changed. The two lines characteristic for the cubic NiO phase (1-1239 JCPDS file) [17], observed for the samples 900N5% and 1100N5% indicate the presence of large size aggregates. They disappear after calcination of the sample at 1400 °C (1400N5%) and its XRD lines (Fig. 6a) become similar to those of the initial olivine calcined at the same temperature (Fig. 6d). This indicates a decrease in the size of nickel containing particles or more probably nickel insertion into the olivine structure.

This study by XRD was completed by other techniques like SEM, TEM coupled with energy dispersive spectroscopy and TPR [13,18]. All these techniques confirm progressive integration of nickel oxide in olivine structure. Three nickel–olivine interaction states were observed at different calcination temperatures. Nickel oxide deposited on the support, weakly linked to olivine, was obtained after calcination at 900 °C and its reduction temperature was low. It was called free nickel oxide (Fig. 7a). After calcination at 1100 °C, nickel oxide forms grafts with the support and these strong nickel–olivine interactions were confirmed by high reduction temperature. In this case, linked nickel oxide reduction is compatible with gasification temperature (Fig. 7b). After calcination at 1400 °C, nickel is integrated into olivine structure, what was confirmed by absence of nickel oxide reduction peak. In this case, nickel was unreachable by reducing gas and was called integrated nickel (Fig. 7c).

3.1.3. Influence of nickel content on the nickel–olivine catalysts

The molar concentration of impregnation solution with nitrate salt was modified in order to obtain catalysts containing from 2 to 10 wt.% of NiO after calcination at 1100 °C. The real nickel content is reported in Table 1. Relative error of these values is about 7%. These results show that efficiency of nickel impregnation was limited when theoretical nickel oxide content

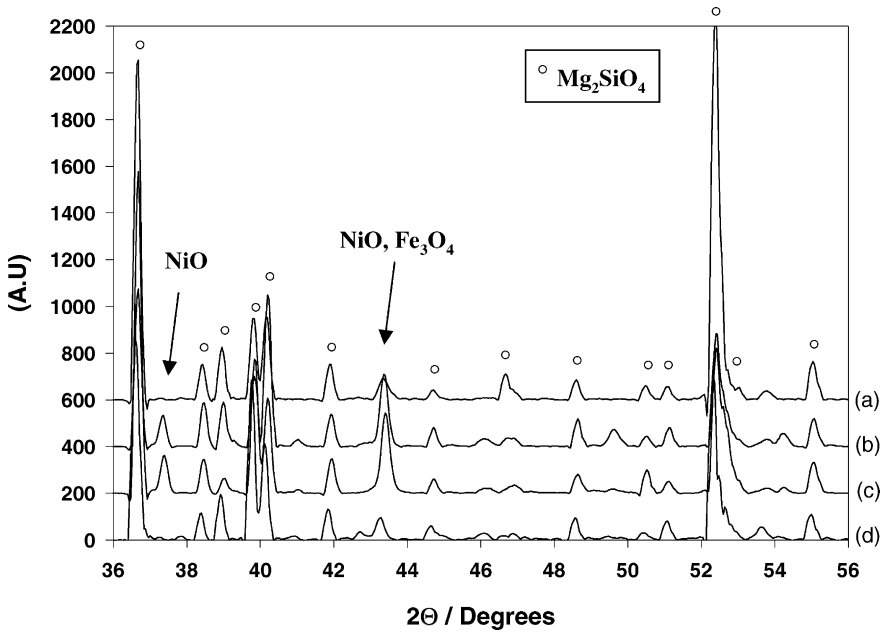

Fig. 6. XRD patterns of (a) 1400N5%, (b) 1100N5%, (c) 900N5% and (d) olivine calcined at 1400 °C.

was higher than 5%. For the samples 1100N5%, 1100N6.4% and 1100N10%, real nickel oxide content varies linearly versus the theoretical value.

These samples were characterised by XRD. Nickel oxide is observed for all samples and the intensity of the corresponding lines increase with increasing content.

The same samples were studied by TPR. The corresponding hydrogen consumption curves were compared (Fig. 8). As foreseen, hydrogen consumption increases with Ni content—the increase of linked nickel oxide reduction peak, with a maximum around 900 °C and increase and widening of reduction peak, with a maximum between 550 and 650 °C is observed. The latter can be attributed to reduction of free (reduction at 450 °C) iron oxide and NiO in different states of interactions with olivine—the intermediate states between free and linked (reduction ∼900 °C) nickel oxide. The presence of free nickel oxide (Fig. 7a) should be avoided because it can lead to carbon formation as well as to the lost of active phase in fluidised bed and then to catalyst deactivation.

3.1.4. Influence of nickel precursor on the nickel–olivine catalysts

In order to study the effect of nickel precursor, samples, 1100N5%, 1100Cl5% and 1100A5% prepared with different salts were characterised. The molar concentration of solutions with various nickel salt was similar in order to obtain catalysts containing 5 wt.% of NiO after calcination at 1100 °C. The real nickel content was determined by elementary analysis and reported in Table 1. Nitrate salt gave the highest nickel oxide content, followed by the chloride salt. 1100A5% sample presents low nickel oxide content. This lack of nickel can be attributed to an inhomogeneous

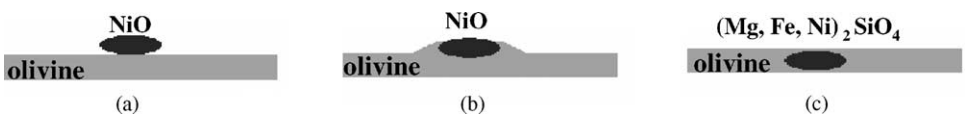

Fig. 7. Nickel–olivine interaction states versus calcination temperature: (a) 900N5%, (b) 1100N5% and (c) 1400N5%.

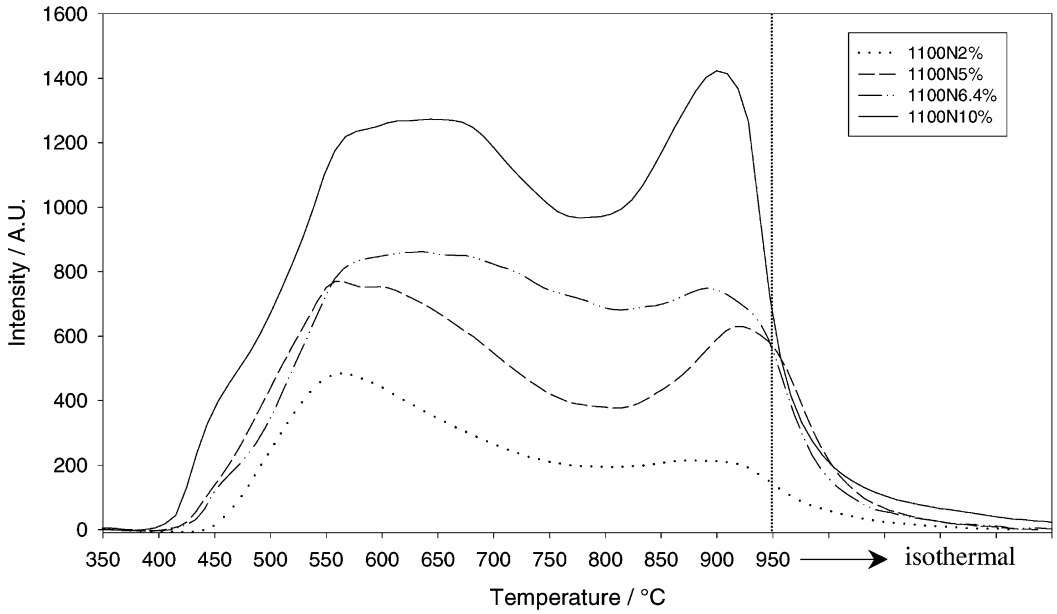

Fig. 8. TPR of 1100N2%, 1100N5%, 1100N6.4% and 1100N10%.

impregnation of nickel acetate on the support due to low solubility of the salt in water.

These samples were characterised by XRD. Nickel oxide is observed on the three samples and no support modification is detected.

TPR was also performed. The different salts lead to the same reduction profile with wide free iron oxide reduction peak (maximum between 560 and 630 °C), followed by linked nickel oxide reduction peak. The only difference is observed for the linked nickel oxide reduction, which takes place at higher temperature for 1100A5% sample (maximum at 920 °C) than for the other ones (maximum at 890 °C).

Taking these results into consideration we can state that, after calcination at 1100 °C nickel oxide is only partially integrated in the olivine structure and part of it is still accessible for reduction on the support surface (Fig. 7b).

3.2. Activity of the nickel–olivine catalysts

3.2.1. Influence of nickel content on the nickel–olivine catalyst activity

Catalysts containing various nickel oxide contents were tested for dry reforming of methane (Fig. 9) with the "cycles and ageing" temperature program (Fig. 2). 1100N2% presents CH_4 conversion with a maximum at 60% and H_2 yield of 55%. The second step at 800 °C (during the second cycle) presents lower values (CH_4 conversion at 55% and H_2 yield at 50%). During the ageing step, a decrease is observed until 15% of methane conversion and 10% of H_2 yield.

1100N5% presents high initial value for CH_4 conversion and H_2 yield (95–90%), but its stability is lower than the 1100N6.4%. 1100N10% presents similar activity and stability (not shown).

The theoretical H_2/CO ratio in dry reforming of methane is equal to 1 (Eq. (1)). During the "cycles and ageing" temperature program, experimental ratio varies with temperature. The theoretical value is obtained at 800 °C during intermediate steps for 1100N5%, 1100N6.4% and 1100N10% samples. For the 1100N2% sample, the highest value obtained is about 0.8 at 800 °C. During ageing at 800 °C, H_2/CO ratio still equal to the theoretical value for 1100N10% and 1100N6.4% samples and becomes stable at 0.9 for 1100N5% sample and at 0.3 for 1100N2% sample.

The decrease in hydrogen production compared with the theoretical one can be associated with carbon dioxide conversion. In fact, in dry reforming of

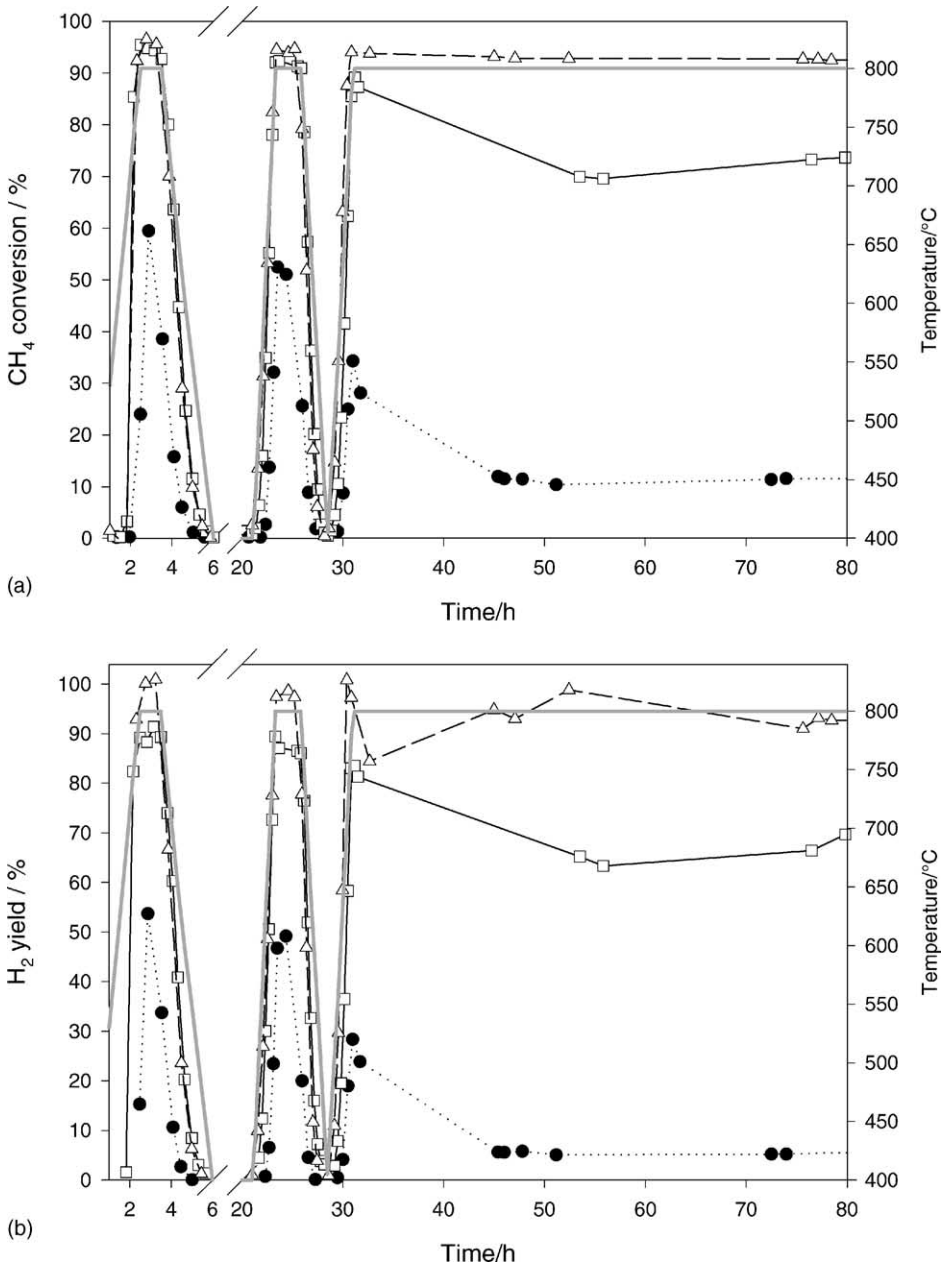

Fig. 9. (a) Methane conversion, (b) hydrogen yield of 1100N6.4% (△), 1100N5% (□) and 1100N2% (●) versus time of stream in dry reforming of methane. Temperature program (—).

methane, methane and carbon dioxide conversions are theoretically equimolar. These equimolar conversions are observed at 800 °C during intermediate steps for 1100N5%, 1100N6.4% and 1100N10% samples. For 1100N2% sample, the highest value of methane to carbon dioxide conversions ratio is about 0.8 at 800 °C. During ageing step, the theoretical methane to carbon dioxide conversions ratio is observed for 1100N10%

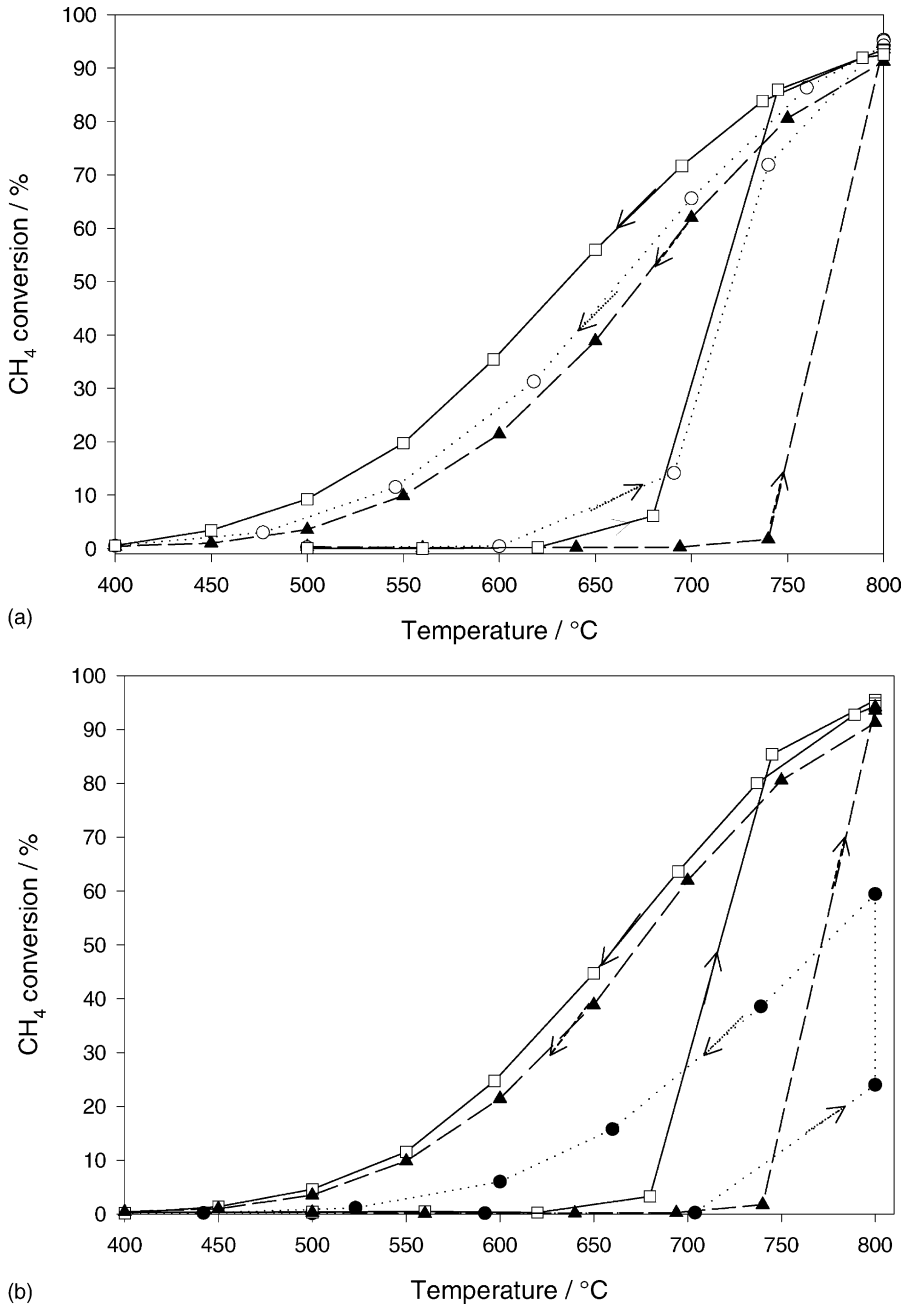

Fig. 10. Methane conversion of (a) 1100N5% (□), 1100Cl5% (○) and 1100A5% (▲); (b) 1100N5% (□), 1100A5% (▲) and 1100N2% (●) versus reaction temperature in dry reforming of methane.

and 1100N6.4% samples and becomes stable at 0.9 for 1100N5% sample and at 0.5 for 1100N2% sample.

Similar changes in H_2/CO ratio and in CH_4/CO_2 ratio are observed. The very low value of H_2/CO ratio associated with the lower CH_4/CO_2 conversions ratio is due to the consecutive reverse water gas shift reaction ($H_2 + CO_2 \rightarrow CO + H_2O$), which is favoured by iron oxide present in the olivine.

Water formed could cover the active sites (Ni^0), reoxidise metallic nickel active phase and then inhibit methane reforming reaction.

3.2.2. Influence of nickel precursor on the nickel–olivine catalyst activity

Catalysts synthesised from various nickel salts were tested (Fig. 10a) with the "simple cycle" temperature regime (Fig. 1). During the increase of temperature, 1100N5% and 1100Cl5% samples are active since 680 °C, 1100A5% sample becomes active at higher temperature (>740 °C). In fact, TPR showed that linked nickel oxide reduction takes place at higher temperature for the 1100A5% sample than for the other ones. On the other hand, sample 1100A5% contains only 3.4 wt.% of NiO and then is also compared with sample 1100N2% (Fig. 10b). Its methane conversion is higher for each temperature of the cycle. In spite of lower Ni content its activity at 800 °C and during the cooling phase is closer to 1100N5%.

Finally, at 800 °C, all samples prepared with various nickel salts present practically the same activity but during the cooling phase, the sample from nickel nitrate is the most active. Experimental H_2/CO ratios are similar for all samples and become stable during ageing at 800 °C with a value of 0.9.

3.3. Characterisation of the nickel–olivine catalysts after catalytic tests

XRD analysis showed that the olivine structure is retained during the different catalytic tests. After dry reforming, NiO phase disappears, Fe_2O_3 and Fe_3O_4 phases decrease and Ni^0 or Ni–Fe alloys with various Ni/Fe ratios were observed. At high initial NiO content, an increase in Ni^0 and Fe–Ni alloys line intensities, a decrease of Fe_3O_4 phase and a disappearance of Fe_2O_3 phase in the "after test" samples are observed. 1100N10% after test presents additional $FeNi_3$ phase, the alloy with the lowest iron/nickel ratio.

Previous work [19] has demonstrated that the formation of Ni–Fe alloys limits coke deposition. TPR of samples after test indicates no hydrogen consumption. All the accessible nickel and iron oxides were reduced during the reactivity tests.

No particle coalescence is observed by SEM of samples after test. Carbon content in the after test samples was determined. Low coke quantity is formed during tests with the "cycles and ageing" temperature program (always lower than 0.5 wt.%).

The calcination at 1100 °C has the advantage to integrate one part of nickel in the support structure and to dispose of one part of nickel reducible on the support surface. The presence of these two nickel species permits to create an equilibrium state with strong interactions between nickel and nickel oxide in the catalyst. These strong nickel–support interactions avoid particle sintering and prevent coke formation.

The state of Ni on the surface associated with the low carbon formation explains good ageing behaviour of the catalysts containing more than 5 wt.% of nickel oxide.

4. Conclusions

Tests of dry reforming of methane have shown that the Ni–olivine catalyst with 6.4 wt.% of nickel oxide on olivine is very active. In addition, this catalyst meets the requirements of high syngas yield and stability with time on stream. In dry reforming of methane with $CH_4/CO_2 = 1$, methane conversion and hydrogen yield reached 95% at 800 °C after the severe conditions of "cycles an ageing" temperature program.

Natural olivine presents good characteristics to be used as biomass gasification catalyst in a fluidised bed reactor but also as nickel support. Iron presence helps in stabilising nickel in reducible conditions. One part of nickel oxide seems to be included into the olivine structure and maintains the reducible nickel oxide on the olivine surface. On the other hand, nickel integration in the olivine structure leads to an increase of free iron oxide, which favours reverse water gas shift reaction.

This catalytic system meets all the requirements of activity, stability and attrition resistance for use in a fluidised bed for biomass steam gasification. It was prepared in large amount and mixed with olivine to

be tested in a pilot plant on a fluidised bed reactor. Excellent performances were observed: difference of gas composition between this bed mixture and olivine alone showed an increase of 8% of hydrogen content and a decrease of 1–3% of the other products. Tar content was very low compared to that obtained with olivine alone. The stability of these results during 50 h and the very low tar content showed no loss of activity of this catalyst [20].

Acknowledgements

The financial support of the E.U. under the contracts JOR3-CT97-0196 and ENK5-CT-2000-00314, is gratefully acknowledged. Authors would like to thank Mrs. G. Ehret and Mr. J. Guille for their collaboration in SEM and TEM.

References

[1] S. Rapagnà, E. Tempesti, A. Kiennemann, P.U. Foscolo, in: Proceedings of the Eighth European Conference on Biomass for Energy, Environment, Agriculture and Industry, October 1994, Vienna, Austria.
[2] J. Corella, M.P. Aznar, J. Delgado, E. Aldea, Ind. Eng. Chem. Res. 30 (1991) 2252.
[3] H. Kubia, H.J. Muhlen, in: Proceedings of the 10th European Conference and Technology Exhibition “Biomass for Energy and Industry”, June 1998, Würztburg, Germany.
[4] H. Hofbauer, T. Fleck, G. Veronik, R. Rauch, H. Mackinger, E. Fercher, in: A.V. Bridgwater, D.G.B. Boocock (Eds.), Developments in Thermochemical Biomass Conversion Conference, Blackie, London 1997, p. 1016.
[5] S. Rapagnà, N. Jand, A. Kiennemann, P.U. Foscolo, Biomass Bioenergy 19 (2000) 187.
[6] S.C. Tsang, J.B. Claridge, M.L.H. Green, Catal. Today 23 (1995) 3.
[7] J. De Deken, P.G. Menon, G.F. Froment, G. Haemers, J. Catal. 70 (1981) 225.
[8] J.H. Larsen, I. Chorkendorff, Surf. Sci. Rep. 35 (1999) 163.
[9] V.R. Choudhary, V.H. Rane, A.M. Rajput, Catal. Lett. 22 (1993) 289.
[10] H.M. Swaan, V.C.H. Kroll, G.A. Martin, C. Mirodatos, Catal. Today 21 (1994) 571.
[11] C. Petit, A. Kiennemann, P. Chaumette, O. Clause, US Patent No. 5,447,705 (1995).
[12] H. Provendier, C. Petit, C. Estournès, S. Libs, A. Kiennemann, Appl. Catal. A 180 (1999) 163.
[13] C. Courson, E. Makaga, C. Petit, A. Kiennemann, Catal. Today 63 (2000) 427.
[14] M. Houalla, F. Delannay, I. Matsuura, B. Delmon, J. Chem. Soc., Faraday Trans. 76 (1980) 2128.
[15] Nat. Bur. Stand (US) Monogr. 25, 20, 71 (1984) JCPDS 34-0189.
[16] A.M. Glazer, Acta Crystallogr. A 31 (1975) 756.
[17] A.M. Huntz, C. Liu, M. Kornmeier, J.L. Lebrun, Corr. Sci. 35 (1993) 988.
[18] C. Courson, C. Petit, A. Kiennemann, J. de Phys. IV 10 (2000) 531.
[19] H. Provendier, C. Petit, C. Estournès, A. Kiennemann, Stud. Surf. Sci. Catal. 119 (1998) 741.
[20] H. Hofbauer, R. Rauch, P.U. Foscolo, D. Matera, in: Proceedings of the First World Conference and Exhibition on Biomass for Energy and Industry, Seville, Spain, June 2000.